Emission Imaging Spectroscopic and Shadowgraphic Studies on the Growth Dynamics of Graphitic Carbon Particles Synthesized by CO_2 Laser Vaporization

F. Kokai,*,† K. Takahashi,† M. Yudasaka,‡ and S. Iijima‡,§,||

Institute of Research and Innovation, 1201 Takada, Kashiwa, Chiba 277-0861, Japan, Nanotubulites Project, JST-ICORP, c/o NEC Corporation, 34 Miyukigaoka, Tsukuba, Ibaraki 305-8501, Japan, NEC Corporation, 34 Miyukigaoka, Tsukuba, Ibaraki 305-8501, Japan, Meijo University, Department of Physics, Tenpaku-ku, Nagoya 468-8502, Japan

Received: May 11, 1999; In Final Form: August 6, 1999

Emission imaging spectroscopy and shadowgraphy were applied to study the growth of carbon particles synthesized by 20-ms CO_2 laser-pulse irradiation at $0.5-1.5 \times 10^5$ W/cm^2 onto a graphite target in an Ar gas atmosphere (300−760 Torr). Emission images of growing carbon clusters and/or particles in a vaporization plume, measured with a temporal resolution of 1.67 ms, showed a constricted structure near the target that expanded widely into the Ar gas environment. On the other hand, the emission images of C_2, not showing the constricted structure, indicated its presence close to the target and expansion in a narrow region. When directly ejected and/or formed carbon species (C, C_2, and C_3 , respectively) with velocities of $0.3-2.6 \times 10^3$ cm/s depart from the graphite surface, the formation of hot carbon clusters and/or particles begins and continues in the expanding plume. In shadowgraph images, the formation of a mushroom cloud containing darkened areas and black spots (size < 1 mm), probably corresponding to ∼80-nm-diameter graphitic carbon particles, was observed after 5 ms from the start of the laser irradiation. The number of particles increased rapidly from 5 to 25 ms. We propose a model of particle growth in a viscous carbon flow, where the temporal and spatial evolution of carbon species (the cluster formation and decrease in kinetic energies) and the condensation of clusters play essential roles with temperature reduction through the interaction with Ar atoms.

Introduction

Carbon particle formation by laser ablation in an inert gas environment is of interest because of its close relationship to the synthesis of fullerenes[1] and single-wall carbon nanotubes (SWNTs).[2] Our recent studies[3,4] on SWNT formation using a 20-ms CO_2 laser and a graphite−Co/Ni (1.2 at %) target in an Ar atmosphere (100−600 Torr) showed that SWNT formation occurred together with carbon and carbon−metal composite particles with diameters of 20−100 nm. The catalytic growth of SWNTs from the carbon−metal composite particles is believed to play an essential role. Furthermore, CO_2 laser vaporization of pure graphite in an Ar atmosphere (760 Torr) at room temperature was found to produce graphitic particles with a uniform diameter of about 80 nm.[5] A magnified transmission electron microscope image showed that the particles were aggregates of tubule-like structures (30- to 50-nm-long nanohorns with a conical cap and an average corn angle of 20 degrees). The morphology of the particles varied with the nanohorns becoming shorter as the laser power density increased. With a further increase in the power density, the particles seemed to be composed of polymerized graphitic cage structures.[6]

Ejection of gaseous carbon species from a graphite surface followed by a clustering reaction and condensation in an inert gas atmosphere leads to the formation of carbon particles. Information on the expansion dynamics of individual carbon species ejected from the target surface and of cluster species formed in a vaporized plume is of particular significance in understanding how various carbon particles are formed. The temporally and spatially dependent growth processes of the particles that take place through the interaction with surrounding inert gas atoms are still not well understood. In this article, we performed laser vaporization of graphite by a 20-ms CO_2 laser pulse in an Ar gas atmosphere at room temperature. The temporal and spatial behaviors of evaporated carbon species and the growth dynamics of carbon clusters and particles were investigated using emission imaging spectroscopy and shadowgraphy. In addition, the vaporization quantity of a graphite target was estimated, and scanning electron microscopy (SEM) was used to examine the target surface after laser irradiation. The emission imaging spectroscopy provided spatially resolved species-specific information on the expanding laser plume. The shadowgraphy, which provides the second derivative of the refractive index distribution in gas-dynamic processes, was used to diagnose the hydrodynamic aspects of laser-ablated materials.[7] We discuss the generation and growth of carbon clusters and particles, composed of aggregates of tubule-like nanostructures,[5] in laser plumes and so-called mushroom clouds that are confined by the Ar gas atmosphere.

Experimental Section

Figure 1a shows our experimental configuration for emission imaging spectroscopy. Laser vaporization was done by focusing a CO_2 laser beam (10.6 μm, 0.4−1.2 kW peak power, 20-ms rectangular pulse) with a ZnSe lens onto a graphite target rod (10 mm in both diameter and length, 1.30 g in weight, 99.99%

* Corresponding author. Telephone: (81) 471-44-8811. Fax: (81) 471-44-8939. E-mail: fkokai@iri.or.jp.
† Institute of Research and Innovation.
‡ Nanotubulites Project, JST-ICORP.
§ NEC Corporation.
|| Meijo University.

10.1021/jp991551i CCC: $18.00
Published on Web 09/23/1999

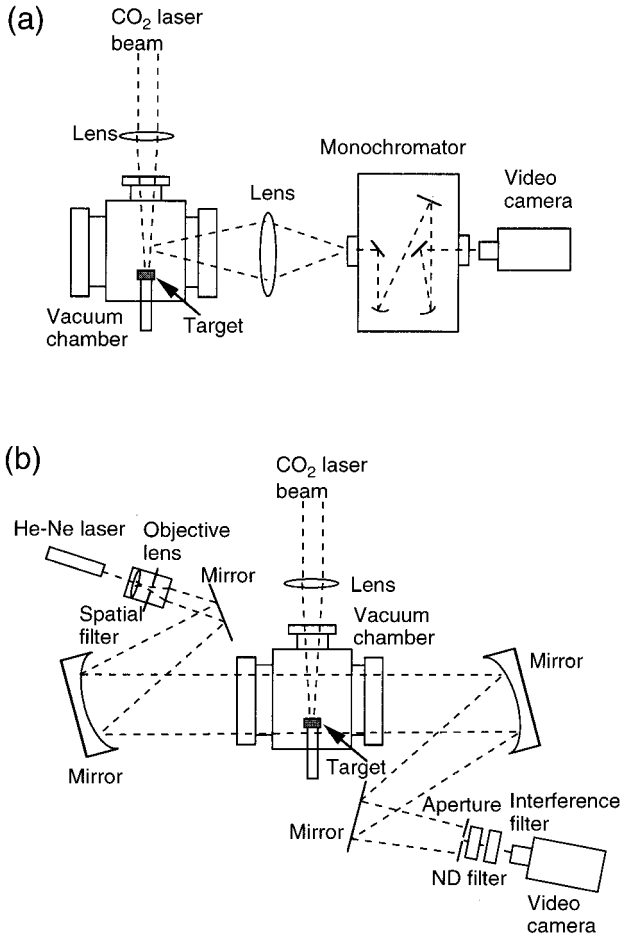

Figure 1. Experimental configurations for time-resolved (a) emission imaging spectroscopy and (b) shadowgraphy.

purity) mounted in a cylindrical stainless steel vacuum chamber (16 cm in diameter and 13 cm long) at room temperature. The chamber was filled with Ar gas at 300−760 Torr. The laser spot size on the graphite surface was 1 mm. The estimated laser power density was in the range of $0.5-1.5 \times 10^5$ W/cm^2. For the irradiation of a single laser pulse on the fresh surface of the graphite target, a series of wavelength-selected images of the side view of an expanding vaporization plume was taken with a monochromator (Nikon P250) and a high-speed video camera (Photron FASTCAM-Rabbit). The Ar gas was exchanged for each measurement. The slit width of the monochromator was 2 mm and the spectral resolution was ∼10 nm. The frame rate of the video camera was 600 s^{-1} and the shutter speed was 10^{-4} s. The temporal resolution of the emission imaging, determined by the frame rate of the video camera, was 1.67 ms. The maximum area of view in the image is 21×4 mm^2.

Figure 1b shows our experimental configuration for the shadowgraphy. Laser vaporization was done in the same way as for the emission imaging spectroscopy. The beam from a He−Ne laser (MELLES GRIOT, 5 mW) passed through a spatial filter and was collimated by two mirrors, then was oriented parallel to the target surface and transversed the plume region. The shadowgraph, corresponding to a side view of the expanding carbon species, was imaged onto the video camera. We used an aperture and an interference filter to suppress the optical emission of the plume. The maximum area of view in the shadowgraph was 68×13 mm^2. The temporal resolution was again 1.67 ms, as determined by the frame rate of the video camera.

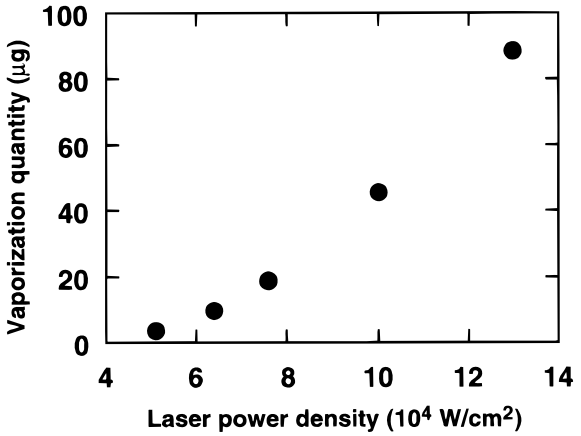

Figure 2. Vaporization quantity of the graphite target as a function of laser power density. The laser vaporization was performed by a single laser pulse in Ar gas at 600 Torr.

After irradiation of a single laser pulse at $0.5-1.3 \times 10^5$ W/cm^2 onto a graphite target, a vaporization quantity from the target was estimated from an etched depth measured by a stylus profilometer (Mitsutoyo Surftest-501). Characterization by SEM of the laser-irradiated surfaces of the targets was done as described in previous papers.[8,9]

Results and Discussion

Vaporization Quantity and SEM Examination of Laser-Irradiated Graphite Surfaces. We first describe the vaporization quantity from a graphite target caused by the irradiation of a single CO_2 laser pulse. Figure 2 shows the vaporization quantity as a function of laser power density at an Ar gas pressure of 760 Torr. For the power density at $0.5-1.3 \times 10^5$ W/cm^2, vaporization quantities ranging from 3.8 to 88.3 μg are obtained. As the power density increases, the vaporization quantity increases nonlinearly. This behavior is probably due to the role of a thermally activated process, where the ejection of carbon species obeys an Arrhenius-type law as has been observed in laser ablation of polymer films.[10]

Figure 3 shows an example of an SEM micrograph of a graphite surface after laser vaporization by a single 20-ms CO_2 laser pulse at 1.3×10^5 W/cm^2. Small sphere-like structures with diameters of 10−20 nm are observed, and these probably result from a melting and resolidification process during and after laser irradiation. However, most of the solid graphite particles in the surface area resemble the original particles before laser irradiation. Similar surface morphologies were observed for the targets after laser irradiation at various power densities. Unlike the SEM micrograph in Figure 3, SEM micrographs of graphite surfaces obtained with nanosecond pulse YAG laser irradiation[3,8,9] showed a clear trace of significant melting in the overall surface area.

Vaporized carbon species expanded at velocities of $\sim 1 \times 10^3$ cm/s during 20-ms CO_2 laser irradiation in an Ar gas atmosphere (600 Torr) in our earlier study,[4] whereas more rapid expansion of carbon species occurs at velocities of $(1-3) \times 10^5$ cm/s with nanosecond pulse YAG laser irradiation in Ar gas at 360−560 Torr.[11] In a laser-vaporization experiment using a nanosecond pulse YAG laser and a pulsed nozzle source,[12] expansion velocities of $\sim 3.4 \times 10^5$ and $\sim 2.0 \times 10^5$ cm/s were measured for C_2 and carbon particles, respectively. These comparisons of the surface morphology and the expansion velocity indicate that the vaporization is slower and milder in

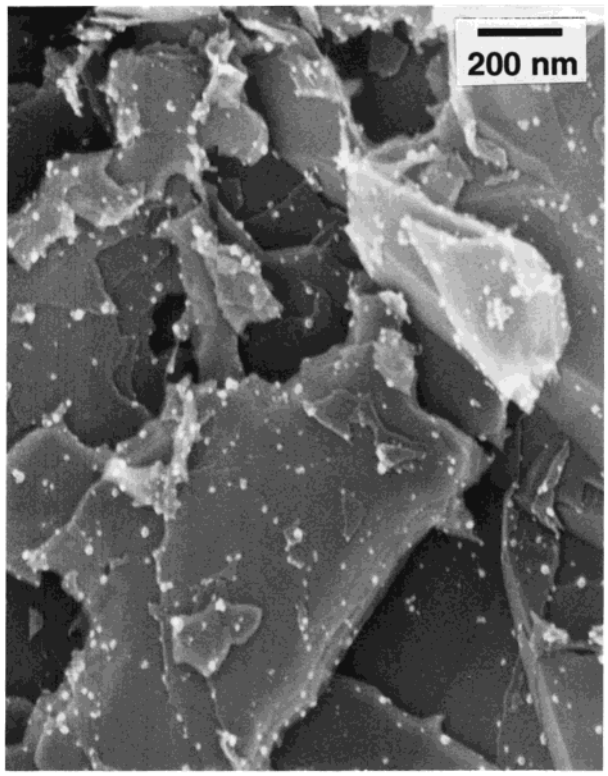

Figure 3. SEM photograph of the graphite target surface after 20-ms CO_2 laser pulse irradiation at 1.3×10^4 W/cm^2 in Ar gas at 600 Torr.

the CO_2 laser irradiation. Compared to ablation with the nanosecond pulse YAG laser via the melting of solid particles throughout the overall surface area, the vaporization process observed here seems to occur at edge regions[3] of the graphite particles. We believe that the major carbon species ejected directly from the graphite surface during CO_2 laser irradiation are carbon atoms and molecular species such as C_2 and C_3. As soon as these carbon species are ejected into the Ar gas atmosphere, significant carbon atom recombination and the growth of larger clusters occur through the interaction with Ar atoms, resulting in the formation of carbon particles as described below. Slow expansion of carbon species during CO_2 laser vaporization is probably favorable for the cluster growth.

Emission Imaging Spectroscopy of C_2 and Carbon Clusters and/or Particles. As in our previous study,[4] a pole-like plume existing for nearly 20 ms was observed during 20-ms pulse CO_2 laser irradiation onto a graphite target in an Ar gas environment. A time-integrated emission spectrum measured for the plume was composed of continuum emission that peaked at 700−800 nm and C_2 Swan band emission. We assigned the continuum emission to that of growing hot carbon clusters and/or particles (blackbody radiation).[11,12] The strongest Swan band was observed at 516 nm. The relative intensity of C_2 emission to that of the continuum emission increased as the Ar gas pressure decreased. For the pole-like plume, time-resolved wavelength-selected emission images were tentatively measured at 516 and 650 nm. The 516- and 650-nm images, obtained at a delay time of 10 ms from the start of CO_2 laser irradiation in Ar gas pressures at 300, 500, and 760 Torr, are shown in Figure 4a−c and Figure 4d−f, respectively. The laser power density was 5×10^4 W/cm^2. In our earlier study,[5] graphitic carbon particles with a diameter of ∼80 nm were grown by laser irradiation at 5×10^4 W/cm^2 in Ar gas at 760 Torr. In addition, Figure 5 shows 516- and 650-nm emission intensities versus the distance normal to the target surface. Each emission intensity

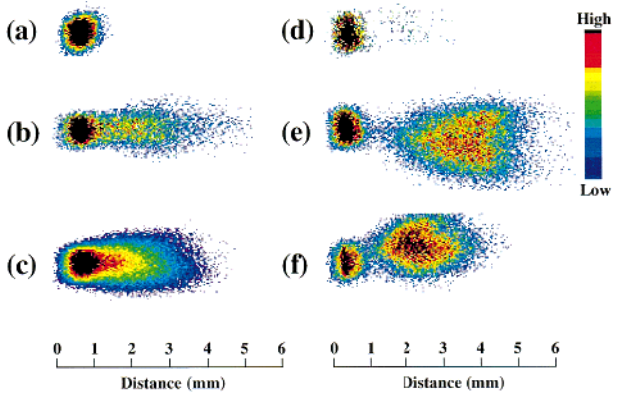

Figure 4. Wavelength-selected emission images obtained at a delay time of 10 ms from the initiation of CO_2 laser pulse irradiation at 5×10^4 W/cm^2 at three Ar gas pressures: (a) 516-nm image at 300 Torr; (b) 516-nm image at 500 Torr; (c) 516-nm image at 760 Torr; (d) 650-nm image at 300 Torr; (e) 650-nm image at 500 Torr; (f) 650-nm image at 760 Torr. The zero point of the scale at the bottom is set to the edge of the emission near the graphite target. The difference in the emission intensity is as shown in the color pallet.

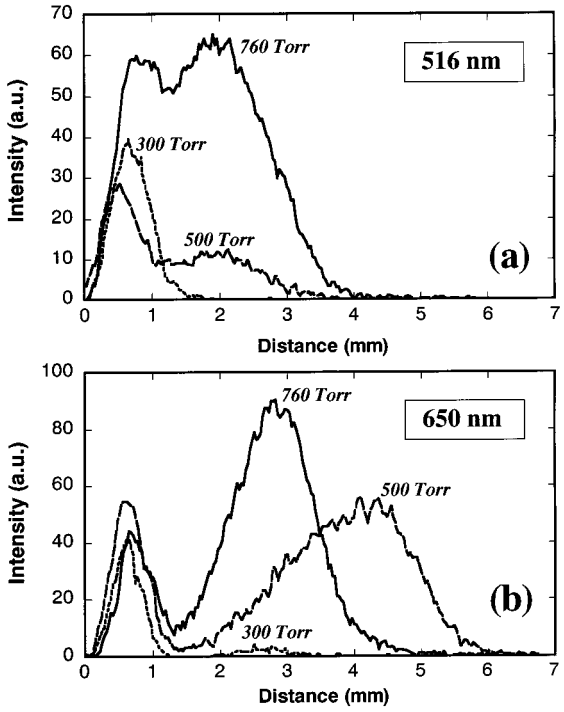

Figure 5. Emission intensity distributions at Ar gas pressures of 300, 500, and 760 Torr versus the distance perpendicular to the target surface in (a) 516- and (b) 650-nm images.

curve was obtained by integrating the emission intensities at the positions along the direction parallel to the target surface in each image in Figure 4.

All images in Figure 4 consist of two parts as most clearly seen in Figures 4e and 4f (see also the two peaks in Figure 5). One part (the image at a distance of > 1 mm) is due to the presence of excited C_2 and growing hot clusters and/or particles expanding into the Ar gas atmosphere. The other part (image at a distance of < 1 mm) is due to the blackbody radiation of the graphite target itself. The emission of C_2 and clusters and/or particles existing near the target also seems to vary the shape of the images at each Ar gas pressure.[14] The emission images at 650 nm (Figure 4d−f), which are due to the presence of the carbon clusters and/or particles, have a constricted part near the target (0.5−1.5 mm from the target) and show distributions

expanding widely in the Ar gas environment. On the other hand, the images at 516 nm (Figure 4a−c) are due to the presence of C_2 and somewhat to the contribution of the continuum emission because of its presence at 300−800 nm. The 516-nm images do not show the distinct constricted structure and are distributed in narrower regions than those of the corresponding 650-nm images. From the noticeable differences between the 516- and 650-nm images for each Ar gas pressure, we believe that the 516-nm images strongly reflect the spatial distribution of C_2. The lengths of the pole-like plumes changed at earlier times (e.g., 0.5−5 mm at 1.7−5.0 ms for a 760-Torr Ar atmosphere) and became constant at 5.0−20.0 ms. However, 516- and 650-nm images with the tendency toward an intensity distribution similar to Figure 4 were obtained at 1.7−20 ms for each Ar gas pressure.[15] As clearly seen in Figure 5, for all Ar gas pressure conditions, the C_2 emission is located in the area close to the target (<4 mm), while the emission of the clusters and/or particles is located further away from the target. Although significant variation in the emission intensities of both C_2 and clusters and/or particles depending on the pressure of Ar gas is seen, larger intensity changes along the distance are observed for the emission of clusters and/or particles.

From the front positions of the plume images at 1.7 and 3.3 ms in Figure 4, we approximately estimated the initial expansion velocities of C_2 and other clusters and/or particles along the direction normal to the target surface. The C_2 velocities are 1.1×10^3 cm/s for 500 Torr and 0.3×10^3 cm/s for 760 Torr. The velocities of other clusters and/or particles are 1.9×10^3 cm/s for 500 Torr and 0.2×10^3 cm/s for 760 Torr. The slower expansion velocities of C_2 and other clusters and/or particles at 760 Torr probably result from more deceleration due to collisions of carbon species with Ar atoms at the interface between the plume and the Ar atmosphere and from the diffusion of Ar atoms into the laser plume.

The lifetime of C_2 Swan band emission is 101.8 ns,[16] corresponding to a moving distance of only $\sim 10^{-6}$ cm in the images estimated from a expansion velocity of $\sim 10^3$ cm/s. For example, at 500 Torr, the C_2 image is distributed within the region of 0−5 mm along the direction perpendicular to the graphite surface (Figure 4b). This is an indication of successive formation and excitation of C_2 in the plume. The presence of the constricted structures in the 650-nm image and their absence in the 516-nm images (Figure 4), and the dependence of the emission intensity distributions on the distance from the target (Figure 5) indicate temporal and spatial differences in the formation and excitation between C_2 and the clusters and/or particles. There must be a distinct formation and excitation of C_2 near the target surface that includes the contribution of carbon atom recombination, the electronic excitation of C_2 ejected directly from the target, etc. When directly ejected and/or formed carbon species (C, C_2, and C_3, respectively) depart from the graphite surface, carbon clusters and/or small particles begin to form and continue forming in the expanding plume. We believe that multibody collision processes, including the contribution of Ar atoms, play an essential role in the growth of the carbon clusters and particles. Two production processes for electronically excited C_2 have been proposed: one is recombinative production from two carbon atoms, and the other is collisional dissociation of large clusters.[12,17] The C_2 emission observed further away from the target (2−4 mm) in Figures 4 and 5 may result from the dissociation of clusters and/or particles. During 20-ms pulse CO_2 laser irradiation, the formation of C_2 and other clusters and/or particles appears to occur steadily.

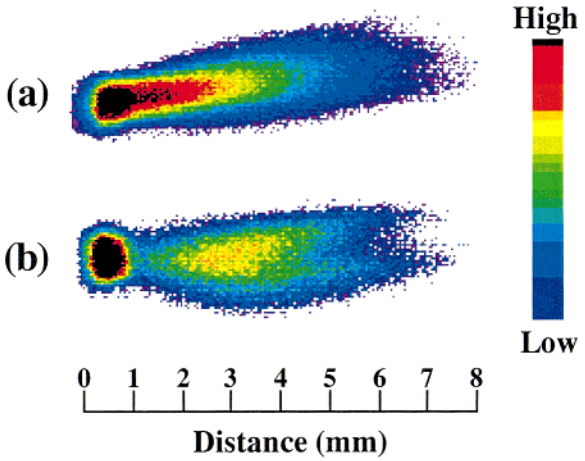

Figure 6. Wavelength-selected emission images obtained at a delay time of 10 ms from the initiation of CO_2 laser irradiation at 1.1×10^5 W/cm^2 at an Ar gas pressure of 760 Torr: (a) 516-nm image; (b) 650-nm image.

For the laser vaporization with higher power densities ($0.8-1.5 \times 10^5$ W/cm^2), we also measured wavelength-selected emission images. With an increasing power density, emission images of longer plumes along the direction perpendicular to the target surface (up to about 10 mm) were obtained for both 516- and 650-nm images (Figure 6). In addition to the constricted structure at 0.5−1.5 mm from the target, the 650-nm image shows a scissors-like structure at the front edge, i.e., a divided structure. The tendency to form the scissors-like structure is also seen in the 650-nm image in Figure 4e. The scissors-like structure may be induced by a dissociation of growing clusters and/or particles into C_2 and other small molecules owing to the incoming CO_2 laser beam. The 516-nm image shows the presence of a large quantity of C_2 species in the gas-phase region near the target. The initial expansion velocities of C_2 and other clusters and/or particles were estimated to be $0.5-2.6 \times 10^3$ cm/s for laser irradiation at $0.8-1.5 \times 10^5$ W/cm^2 in an Ar gas atmosphere of 760 Torr. This indicates much faster expansion than that at 5×10^4 W/cm^2 (Figure 4).

Shadowgraphy of Laser Plumes and Carbon Particles. Through the measurement of shadowgraph images at various times after the initiation of laser irradiation, we observed carbon species, including particles, moving in a viscous flow. Figure 7 shows such a series of shadowgraph images acquired at various times (3.3−45.0 ms) from the initiation of 20-ms CO_2 laser pulse irradiation at 5×10^4 W /cm^2 in Ar gas at 760 Torr (corresponding to the formation condition of ~80-nm-diameter graphitic particles). The shadowgraph images at 3.3−20.0 ms show the continuous ejection of carbon species from the target and the formation and growth of a mushroom cloud, composed of sphere-like and long tail parts, in the Ar gas atmosphere. The widths of the tail clouds are 5−10 mm at 8.3 and 11.7 ms, while the widths of emission images in Figure 4c and 4f are less than 2 mm. It is likely that the outside region of the mushroom cloud is Ar gas compressed by the expanding carbon species. In the mushroom cloud, the darkened parts and black spots (size < 1 mm) are inhomogeneously distributed over the cloud region of > 5 mm from the target. We think the darkened parts and black spots, generated by scattering and absorption of He−Ne laser light, correspond to a large number of carbon particles. As seen in the images at 5.0−20.0 ms, carbon particles appear to grow in both the sphere-like and the tail parts of the clouds. As time increases, the sphere-like cloud moves forward and becomes larger as a result of the increase in the number of particles. During the continuous ejection of carbon species from

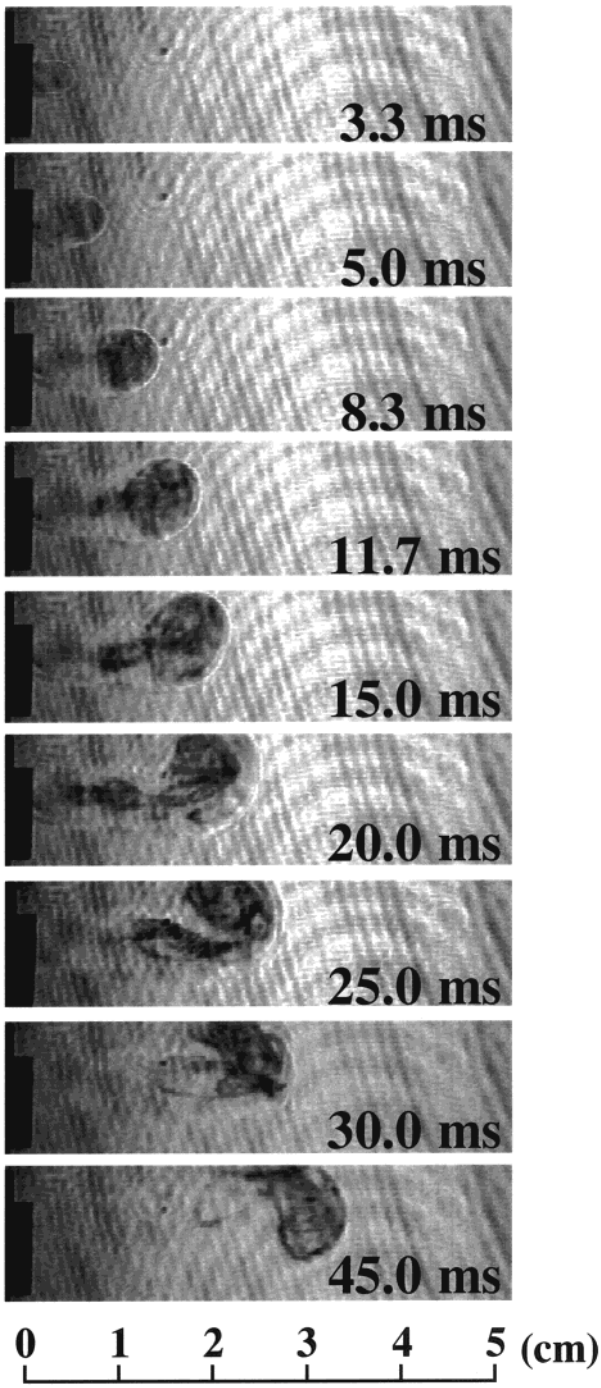

Figure 7. Series of shadowgraph images at 3.3, 5.0, 8.3, 11.7, 15.0, 20.0, 25.0, 30.0, and 45.0 ms from the start of irradiation with a 20-ms CO_2 laser pulse onto graphite at 5×10^4 W/cm^2 in Ar gas at 760 Torr. The CO_2 laser was incident from the right of the image, perpendicular to the target surface. A length scale is shown in the bottom of the images.

the target for ~20 ms, the formation of particles with diameters detectable by shadowgraphy begins to occur in the central region of the tail cloud. The formation begins at > 5 mm from the target, because of the temperature reduction of vaporized carbon species as they depart from the target. The formed particles in the tail cloud appear to propagate into the sphere-like cloud. We also examined moving video pictures of the shadowgraphs and found that the darkened area and the number of black spots increased in the sphere-like cloud, and both moved around in a vortex motion,[18] which is a well-known phenomenon in fluid dynamics. During the ejection of carbon species from the target, the darkened areas and black spots were continuously emitted in the tail cloud (> 5 mm from the target). After the end of laser irradiation, as shown in the shadowgraph images at 25.0, 30.0, and 45.0 ms in Figure 7, the sphere-like part of the mushroom cloud moves forward very slowly. The tail part becomes folded with the sphere-like part. As time increases further, the sphere-like and tail parts mixes together. This occurs because the sphere-like cloud decelerates earlier and the tail cloud maintains its kinetic energy because of the later departure of carbon species from the graphite target.

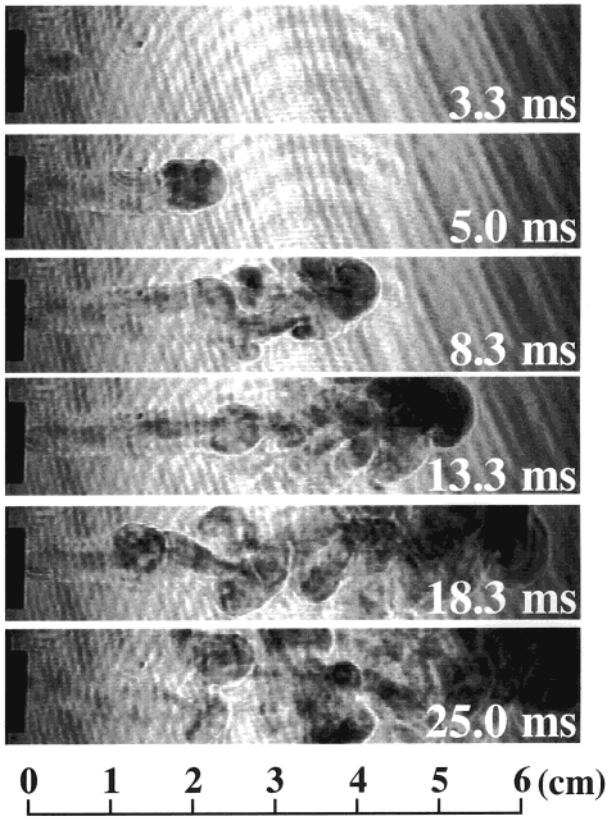

Figure 8. Series of shadowgraph images at 3.3, 5.0, 8.3, 13.3, 18.3, and 25.0 ms from the start of the irradiation with a 20-ms CO_2 laser pulse onto graphite at 1.0×10^5 W/cm^2 in Ar gas at 760 Torr.

A significant increase in the darkened areas and the number of the black spots in the mushroom cloud takes place from 5 to 25 ms in Figure 7. We believe that the particle detected by the shadowgraphy correspond to a large number of ~80-nm diameter graphitic particles[5] and that the number of particles increases significantly at 5−25 ms. This is consistent with the video observation of soot-like materials appearing at > 3 ms from the initiation of CO_2 laser irradiation in our earlier study.[4] Compared to the position of the emission images of carbon clusters and/or particles in Figure 4 (<6 mm from the target), the particles detected by the shadowgraphy are located further from the target. We think that the hot particles detected by emission imaging spectroscopy become larger via collisions with carbon clusters, their temperatures fall, and they become detectable with shadowgraphy.

With increasing laser power density, the shadowgraph images showed a drastic change in the formation of the mushroom cloud. Figure 8 shows a series of shadowgraph images obtained for laser irradiation at 1.0×10^5 W/cm^2 in Ar gas at 760 Torr (corresponding to the formation condition for polymerized graphitic cage structures[5]). The laser power density was doubled compared to the images in Figure 7. The image at 5.0 ms in Figure 8 shows a carbon particle detected at a position 15−20

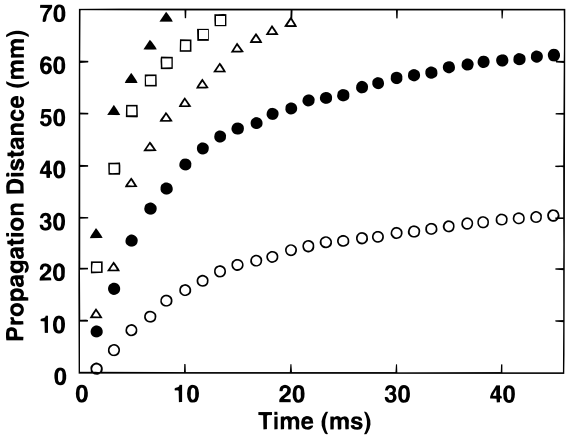

Figure 9. Plot of the propagation distance of the front edge of the mushroom cloud as a function of the time from the initiation of the laser irradiation. Laser power densities were (○) 5.1×10^4, (●) 7.6×10^4, (△) 1.0×10^5, (□) 1.3×10^5 , and (▲) 1.5×10^5 W/cm^2.

mm from the target. This is much farther from the target than in Figure 7. The position is probably determined by the interaction between carbon species ejected with higher velocities and temperatures and diffusing Ar atoms. In addition, during the steady ejection of carbon species from the target for nearly 20 ms, the formation of many turbulent clouds containing particles is also observed. This behavior is similar to the transition from laminar to turbulent flow at a definite value of Reynolds number. The instability taking place at the interface between the plume and the ambient Ar gas probably causes mixing between carbon species and Ar atoms by enfolding the Ar atoms and then inducing the formation of the turbulent clouds. Compared to the formation of the mushroom cloud in Figure 7, the cloud formation here occurs in a much wider space and the formed clouds propagate at higher velocities.

Figure 9 shows the propagation distance of the front edge of the mushroom cloud as a function of the time after the start of the laser irradiation. The laser power densities range from 0.5×10^5 to 1.5×10^5 W/cm^2. At all power densities, the propagation distance from the target increases most rapidly within the first 10 ms. As the time increases further, only a slight increase in the distance is observed. This behavior is related to collisions of the carbon species with Ar atoms and the diffusion of Ar atoms into the mushroom cloud, which both decelerate the carbon species. Finally, carbon particles drift in the Ar gas atmosphere after losing much of their kinetic energy. For example, at a power density of 5×10^4 /cm^2, the expansion velocities estimated from the propagation distances are 2.2×10^2 cm/s at 1.7−3.3 ms, 1.1×10^2 cm/s at 10.0−11.7 ms, 40 cm/s at 21.7−23.3 ms, 4 cm/s at 28.3−30 ms, and 1 cm/s at 43.3−45.0 ms. With increasing laser power density, faster propagation of the cloud is observed. This is probably due to the higher initial velocities of the C, C_2, and C_3 species vaporized from the graphite surface.

We also observed that the size of the mushroom cloud and its development over time varied significantly depending on the pressure of the surrounding Ar gas. Figure 10 shows shadowgraph images acquired at Ar gas pressures of 300−760 Torr. The laser power density was 5×10^4 W/cm^2 and the delay time for the measurement of the image was 10 ms for each image. With increasing pressure, the mushroom cloud propagates more slowly with a narrower tail and smaller sphere-like parts. The smaller sphere-like cloud contains more darkened areas and black spots, indicating the growth of carbon particles with higher densities. Figure 11 shows the distance of the front edge of the

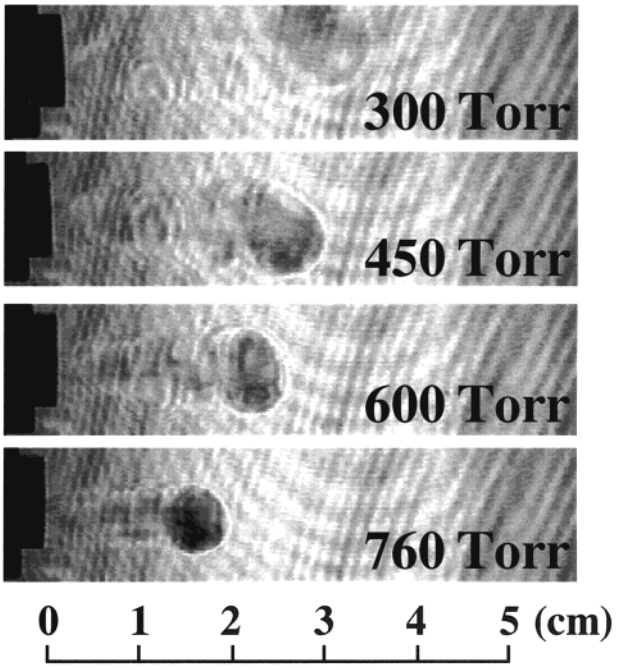

Figure 10. Shadowgraph images at Ar gas pressures of 300−760 Torr. The laser power density is 5×10^4 W/cm^2 and the delay time for the measurement of the image was 10 ms for each image.

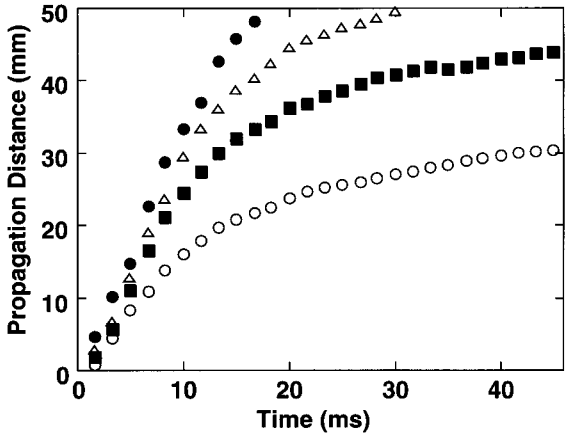

Figure 11. Plot of the propagation distance of the front edge of the mushroom cloud as a function of the time from the initiation of the laser irradiation. Ar gas pressures were (●) 300, (△) 450, (■) 600, and (○) 760 Torr.

mushroom cloud as a function of time after the initiation of laser irradiation in Ar gas pressures of 300−760 Torr. With increasing pressure, slower propagation is observed. The difference in the propagation velocity depending on the Ar gas pressure becomes large after 10 ms. It is most likely that the accumulated deceleration due to successive collisions of carbon species with Ar atoms causes the large difference in the propagation distance with increasing time.

Model of Particle Growth in a Viscous Flow. We propose here a model of particle growth in a viscous carbon flow, where the temporal and spatial evolution of carbon species (the cluster formation and decrease in kinetic energy) and their temperature reduction with the interaction with Ar atoms play essential roles in the growth of carbon particles. First, the irradiation of a 20-ms laser pulse onto a graphite target causes the ejection of gaseous carbon species (C, C_2, and C_3) with flight velocities of 10^2-10^3 cm/s, and these species form a viscous flow in an Ar gas atmosphere. Second, as soon as the ejection begins, the formation and growth of carbon clusters starts, because of

collisions among the carbon species in a laser plume (3−20 mm in length depending on the laser power density) confined by Ar gas atoms. This formation and growth of the carbon clusters is followed by a condensation process to form particles with relatively high temperatures (3400−3500 K)[4] emitting blackbody radiation. Third, when the hot clusters and particles propagate further into the Ar atmosphere, a mushroom cloud composed of a sphere-like and a tail part is formed (> 8 mm from the target and ∼5 ms from the start of laser irradiation) and becomes larger. It is most likely that rearrangement of carbon atoms takes place easily to form a stable graphitic structure in the high-temperature carbon particles. Further growth of the carbon particles (up to ∼80 nm) occurs through the collisions between carbon clusters and condensed particles with a vortex phenomenon in the sphere-like cloud. Fourth, during the steady ejection of carbon species from the target for nearly 20 ms, a continuous formation of particles also occurs in the tail cloud and these particles propagate into the spherical cloud. The number of particles significantly increases from 5 to 25 ms. During the particle formation, cooling and deceleration processes take place involving small carbon species, clusters, and particles through the interaction with Ar atoms, together with the successive diffusion of surrounding Ar atoms into the sphere-like and tail clouds. In addition, at higher laser power densities, instability causes mixing of carbon species and Ar atoms, leading to the formation of turbulent clouds. We believe that the growth velocities and the yield of various carbon particles are strongly dependent on the feature of laser plumes. The feature is determined by the vaporized carbon species (quantities, kinetic energies, and temperatures) and the ambient Ar gas (confinement and diffusion processes dominated by the pressure).

Concerning the formation of various carbon particles depending on the laser power density,[5] we analyzed the experimental results obtained for power densities of 5×10^4 (corresponding to the formation of graphitic particles with a diameter of ∼80 nm) and 1×10^5 W/cm^2 (corresponding to the formation of particles with polymerized graphitic cage structures) in an Ar atmosphere of 760 Torr. The vaporization quantities of the graphite target are 3.8 and 45.6 μg for 5×10^4 and 1×10^5 W/cm^2, respectively (Figure 2). The estimated area of the mushroom and turbulent clouds at 25 ms in Figure 8 (1×10^5 W/cm^2) is roughly five times larger than that of the mushroom cloud at 25 ms in Figure 7 (5×10^4 W/cm^2). Consequently, the estimated volume of the cloud in Figure 8 is 11.8 times that of the cloud in Figure 7. A comparison of the vaporization quantities and the cloud volumes indicates that the densities of carbon atoms in the two clouds are almost the same, although the ratio of clusters to particles present and the structures of the particles are probably different in the two clouds. On the other hand, the difference in the laser power density leads to the ejection of carbon species with significantly different initial velocities, 2.2×10^2 cm/s at 5×10^4 W/cm^2 and 5.4×10^2 cm/s at 1×10^5 W/cm^2 (Figure 9), resulting in the differences in the velocity and frequency of collisions associated with the formation of carbon clusters and particles. We suggest that the initial kinetic energies of carbon species are responsible for the formation and growth of the two kinds of carbon particles. The formation of graphitic particles with a diameter of ∼80 nm may be the result of a slow particle growth process.

Conclusion

CO_2 laser vaporization of graphite can produce structurally different carbon particles in an Ar gas atmosphere. We have diagnosed the vaporization carbon plume and the carbon particles using emission imaging spectroscopic and shadowgraphic techniques. Using emission imaging spectroscopy, the temporally and spatially dependent behaviors of excited C_2 and growing hot carbon clusters and/or particles were revealed in the expanding laser plume produced by 20-ms laser pulse irradiation. Shadowgraphy enabled us to visualize the growth of the large carbon particles, which occurred with the formation of a mushroom cloud with reducing temperature. We concluded that the number of the ∼80-nm-diameter graphitic carbon particles increased rapidly from 5 to 25 ms after the start of laser irradiation. The growth dynamics of the carbon particles, which strongly depend on both laser power density and Ar gas pressure, should be analyzed in terms of multiple factors, including expansion velocities and collisions of carbon species, interaction with surrounding Ar atoms, and condensation of carbon clusters. In addition, the formation of vortex and turbulent flow, which are familiar phenomena of fluid dynamics, should also be considered.

Finally, we proposed a model of particle growth in a viscous flow. In the model, the temporal and spatial evolution of carbon species and the condensation of carbon clusters play essential roles in the particle formation. Furthermore, structural rearrangement resulting in a graphitic structure is expected to occur when the particles are still hot enough to allow the movement of carbon atoms in the particles. The diffusion of Ar atoms occurs at the interface between the Ar atmosphere and both the sphere-like and tail parts in the mushroom cloud, and it causes mixing between the carbon clusters/particles and Ar atoms leading to the temperature reduction of the carbon clusters/particles. For the particle formation at a constant Ar gas pressure, we suggested that control of the kinetic energies of carbon species ejected from a graphite target led to the formation of various carbon particles.

Although the CO_2 laser vaporization of graphite can produce graphitic carbon particles with a uniform diameter of about 80 nm, more work, such as investigation of the size and temperature distributions of the hot carbon clusters and particles in the sphere-like and tail clouds, is needed to clarify the growth dynamics of the particles in detail.

References and Notes

(1) Kroto, H. K.; Heath, J. R.; O'Brien, S. C.; Curl, R. F.; Smalley, R. E. *Nature* **1985**, *318*, 162.

(2) Iijima, S.; Ichihashi, T. *Nature* **1993**, *363*, 603.

(3) Yudasaka, M.; Kokai, F.; Takahashi, K.; Sensui, N.; Iijima, S. *J. Phys. Chem. B* **1999**, *103*, 3576.

(4) Kokai, F.; Takahashi, K.; Yudasaka, M. R.; Yamada, R.; Iijima, S. *J. Phys. Chem. B* **1999**, *103*, 4346.

(5) Iijima, S.; Yudasaka, M.; Yamada, R.; Bandow, S.; Suenaga, K.; Kokai, F.; Takahashi, K. *Chem. Phys. Lett.* **1999**, *309*, 165.

(6) Iijima, S.; Wakabayashi, T.; Achiba, Y. *J. Phys. Chem.* **1996**, *100*, 5839.

(7) Ventzek, P. L. G.; Gilgenbach, R. M.; Ching, C. H.; Lindley, R. A. *J. Appl. Phys.* **1992**, *72*, 1696.

(8) Yudasaka, M.; Komatsu, T.; Ichihashi, I.; Iijima, S. *Chem. Phys. Lett.* **1998**, *278*, 102.

(9) Yudasaka, M.; Komatsu, T.; Ichihashi, T.; Achiba, Y.; Iijima, S. *J. Phys. Chem. B* **1998**, *102*, 4892.

(10) Kokai, F.; Niino, H.; Yabe, A. *J. Phys. Chem.* **1998**, *102*, 8400.

(11) Kokai, F.; Takahashi, K.; Shimizu, K.; Yudasaka, M.; Iijima, S., unpublished results.

(12) Rohlfing, E. A. *J. Chem. Phys.* **1988**, *89*, 6103.

(13) Geohegan, D. B.; Puretzky, A. *Mater. Res. Symp. Proc.* **1996**, *397*, 55.

(14) Expansion of evaporated species from a target in an inert gas environment is fairly slow because of the recoil of the evaporated species caused by inert gas atoms. For example, evaporated Al species are still in contact with an Al target surface at 47 μs after nanosecond pulse excimer laser ablation in Ar gas at 250 Torr (ref 7), in which ablated Al species are

expected to receive higher expansion velocities than those of the carbon species observed in our study.

(15) We believe that a time period of 1.7 ms is long enough to form hot clusters and/or particles. In ref 12, a similar continuum emission that peaked at 750 nm was observed at 57 μs after laser vaporization of graphite using a nanosecond pulse Nd:YAG laser.

(16) Naulin, C.; Costes, M.; Dorthe, G. *Chem. Phys. Lett.* **1988**, *143*, 496.

(17) Anselment, M.; Smith, R. S.; Daykin, E.; Dimaruo, L. F. *Chem. Phys. Lett.* **1987**, *134*, 444.

(18) Sappey, A. D.; Gamble, T. K. *J. Appl. Phys.* **1992**, *72*, 5095.